Biochemistry and Biophysics Reports 27 (2021) 101034

Contents lists available at ScienceDirect

Biochemistry and Biophysics Reports

journal homepage: www.elsevier.com/locate/bbrep

Stability of human salivary extracellular vesicles containing dipeptidyl peptidase IV under simulated gastrointestinal tract conditions

Yuko Ogawa [a,*], Yoshihiro Akimoto [b], Mamoru Ikemoto [a], Yoshikuni Goto [a], Anna Ishikawa [a], Sakura Ohta [a], Yumi Takase [a], Hayato Kawakami [b], Masafumi Tsujimoto [a], Ryohei Yanoshita [a]

[a] Faculty of Pharmaceutical Sciences, Teikyo Heisei University, 4-21-2 Nakano, Nakano-ku, Tokyo, 164-8530, Japan
[b] Department of Anatomy, Kyorin University School of Medicine, 6-20-2 Shinkawa, Mitaka, Tokyo, 181-8611, Japan

ARTICLE INFO

Keywords:
Extracellular vesicles
Exosomes
Stability
Human whole saliva
Dipeptidyl peptidase IV
Gastrointestinal condition

ABSTRACT

Background: Extracellular vesicles (EVs) have been isolated from various sources, including primary and cultured cell lines and body fluids. Previous studies, including those conducted in our laboratory, have reported the stability of EVs under various storage conditions.

Methods: EVs from human whole saliva were separated via size-exclusion chromatography. To simulate the effects of gastric or intestinal fluids on the stability of EVs, pepsin or pancreatin was added to the samples. Additionally, to determine the effect of bile acids, sodium cholate was added. The samples were then subjected to western blotting, dynamic light scattering, and transmission electron microscopy analyses. In addition, the activity of dipeptidyl peptidase (DPP) IV retained in the samples was examined to monitor the stability of EVs.

Results: Under acidic conditions, with pepsin mimicking the milieu of the stomach, the EVs remained stable. However, they partially lost their membrane integrity in the presence of pancreatin and sodium cholate, indicating that they may be destabilized after passing through the duodenum. Although several associated proteins, such as mucin 5B and CD9 were degraded, DPP IV was stable, and its activity was retained under the simulated gastrointestinal conditions.

Conclusion: Our data indicate that although EVs can pass through the stomach without undergoing significant damage, they may be disrupted in the intestine to release their contents. The consistent delivery of active components such as DPP IV from EVs into the intestine might play a role in the efficient modulation of homeostasis of the signal transduction pathways occurring in the gastrointestinal tract.

1. Introduction

Extracellular vesicles (EVs) of diameters less than 200 nm are often referred to as “exosomes” and are secreted from various cell types, including reticulocytes, lymphocytes, dendritic cells, and intestinal epithelial cells. They are also present in various body fluids, including blood, breast milk, malignant ascites, urine amniotic fluid, and saliva. Exosomes are defined as EVs released into the extracellular milieu upon the fusion of multi-vesicular bodies (MVB) with the cell plasma membrane [1]. EVs/exosomes may contain proteins and nucleic acids from the cells in which they were formed and can transfer their contents to target cells upon fusion [2]; hence, they are involved in intercellular communication via the delivery of their cargo.

It has been reported that EVs derived from breast cancer cells interact with salivary gland cells to alter the protein and mRNA compositions of salivary gland-originated EVs [3]. For instance, in patients with oral lichen planus, a chronic inflammatory oral mucosal disease, the miR-4484 levels in salivary exosomes are significantly increased [4]. Additionally, we have previously reported that inflammatory stimuli could change the composition and function of exosome-like vesicles secreted from RAW264.7 cells [5]. These results imply that EV/exosome-secreting cells can change the contents of their EVs/exosomes depending on the milieu they are exposed to and thus modulate pathophysiological processes in the body.

Abbreviations: Alix, programmed cell death 6-interacting protein; DLS, dynamic light scattering; DPP IV, dipeptidyl peptidase IV; EVs, extracellular vesicles; MCA, 4-methyl-coumaryl-7-amide; PBS, phosphate buffered saline; PLA_2, phospholipase A2; SD, standard deviation; TEM, transmission electron microscopic; TSG101, tumor susceptibility gene 101; WS, whole saliva.

* Corresponding author.
E-mail address: y.ogawa@thu.ac.jp (Y. Ogawa).

https://doi.org/10.1016/j.bbrep.2021.101034
Received 25 December 2020; Received in revised form 21 May 2021; Accepted 21 May 2021

Human saliva plays an important role as a front-line defense system of the body through its lubricating, antibacterial, antiviral, and buffering actions. It also helps to moisten and partly digest food. Saliva is an aqueous complex of proteins, peptides, metabolites, DNA, RNA, and minerals. Previously, we reported that human whole saliva (WS) contains at least two types of EVs, one of which was recognized as exosomes based on the expression of several proteins, including the tetraspanins CD9 and CD63, and the cytosolic proteins programmed cell death 6-interacting protein (Alix) and tumor susceptibility gene 101 (TSG101), which are well-recognized exosome markers [6]. Additionally, we have also previously identified EVs/exosome-like vesicles containing dipeptidyl peptidase IV (DPP IV) in both snake venom (*Gloydius blomhoffii*) [7] and human WS [8]. Based on these results, we proposed DPP IV as one of the membrane markers of salivary EVs [9]. DPP IV is a ubiquitous type II transmembrane serine peptidase present in all organisms from bacteria to mammals. It cleaves proline- or alanine-ending dipeptides (from the N-terminus end) [10], including glucagon-like peptide-1 and glucose-dependent insulinotropic peptide. Therefore, DPP IV inhibitors are commonly used to treat type 2 diabetes. In fact, placental extracellular vesicles express DPP IV, whose activity is increased in gestational diabetes mellitus [11]. In addition, the expression of DPP IV is decreased in children with celiac disease, an autoimmune disease in which ingestion of gluten damages the small intestine [12]; owing to the high proline content of gluten, DPP IV is one of the enzymes that contribute to its digestion [13]. Since human salivary EVs are associated with membrane-bound DPP IV, we hypothesized that DPP IV in salivary EVs may not only be used as an indicator of the stability of salivary EVs but also have pathophysiological relevance.

In a previous study, we reported that salivary EVs/exosomes are quite stable, retaining their membrane integrity for a long time when stored at 4 °C [9]. Several studies in the context of EVs/exosomes derived from urine, plasma, and milk samples also found that their protein and microRNA contents were highly stable under a variety of storage conditions [14]. In addition, Liao et al. reported that microRNAs in milk exosomes remained intact during gastrointestinal passage [15]. Since salivary EVs transit through the gastrointestinal tract after being secreted from the salivary glands, it is important to determine their stability against digestive enzymes to elucidate their pathophysiological significance.

Therefore, in this study, we evaluated the stability and integrity of salivary EVs under simulated gastrointestinal tract conditions using digestive enzymes and bile acids and evaluated the morphology of EVs and the degradation of their protein components. Overall, our results indicated that salivary EVs can pass through the stomach without undergoing significant damage but are probably disrupted in the intestine to release their contents.

2. Materials and Methods

2.1. Materials

Gly-Pro-4-methyl-coumaryl-7-amide (Gly-Pro-MCA) was purchased from Peptide Institute Inc. (Osaka, Japan). Sephacryl S-500 HR was purchased from GE Healthcare UK Ltd. (Buckinghamshire, UK). For electron microscopy sample preparation, 25% glutaraldehyde (G011/1) was purchased from TAAB Laboratories Equipment Ltd. (Berkshire, England) and collodion support film on 200 mesh copper grids (No. 6511) was purchased from the Nisshin EM Corporation (Tokyo, Japan). The digestive enzymes pepsin (P7000) and pancreatin (163-00142) were purchased from Sigma-Aldrich (St. Louis, MO, USA) and FUJIFILM Wako Pure Chemical Corporation (Osaka, Japan), respectively. Recombinant human DPP IV (rhDPP IV) (1180-SE-010) was purchased from R&D Systems, Inc. (Minneapolis, MN, USA). The detergents, sodium cholate (C1254) and the protease inhibitor cocktail (S8820, SIGMAFAST Protease Inhibitor Tablets), were purchased from Sigma-Aldrich (St. Louis, MO, USA). All other reagents used were of the highest quality available.

2.2. Isolation of EVs from human WS

Ethical approval was obtained from the institutional review board of Teikyo Heisei University (approval number R01-109). Human WS was collected from 13 healthy volunteers from our laboratory aged between 22 and 49 years (donors A–M) after obtaining written informed consent. EVs were purified from the WS as previously described, with minor modifications [6]. Briefly, 40 mL of WS was added to an equal volume of Tris-buffered saline (20 mM Tris-HCl, pH 7.4 and 150 mM NaCl) and subjected to centrifugation at 6,000×*g* for 15 min at 20 °C (himac CF16RXII; T9A31 rotor; Koki Holdings Co., Ltd. Tokyo, Japan) to remove cell debris and bacteria as the pellet. The supernatant was filtered through a 5.0-μm cellulose acetate filter (17594-K, Sartorius, Göttingen, Germany) and concentrated to approximately 1 mL in an Amicon Ultra-15 centrifugal filter device with a 100 kDa exclusion (Millipore Corporation, Bedford, MA, USA). The concentrated filtrate was then purified using gel filtration chromatography on a Sephacryl S-500 HR column (1.5 × 50 cm, 0.33 mL/min) equilibrated with Tris-buffered saline (pH 7.4), and 110 fractions were collected (Fraction collector FC204, Gilson, Middleton, WI, USA) within 6 h. The absorbance of all fractions at 280 nm and the DPP IV activity were analyzed; fractions corresponding to a small peak of absorbance with high DPP IV activity were pooled and filtered through a 0.2-μm cellulose acetate filter (2062-025, AGC TECHNO GLASS Co, Ltd., Shizuoka, Japan). The pooled fractions were concentrated and exchanged into phosphate-buffered saline (PBS, pH 7.4) using Amicon Ultra-4 with a 100 kDa exclusion. The protein concentration of the fractions was determined using the Pierce™ BCA Protein Assay Kit (23235, Thermo Fisher Scientific, Waltham, MA, USA) according to the manufacturer's instructions. The concentrated fractions were also used for further characterization. Isolated EV fractions were stored at 4 °C until further use. All relevant data in this study have been submitted to the EV-TRACK knowledgebase (EV-TRACK ID: EV200078) [16].

2.3. DPP IV activity assay

DPP IV activity was assayed as previously described [8]. Briefly, assay mixtures containing 50 μL of 0.4 mM Gly-Pro-MCA, 100 μL of 100 mM Tris-HCl (pH 8.5), and 50 μL of enzyme solution were prepared. After incubation for 20 min at 37 °C, 2.8 mL of 1 M sodium acetate (pH 4.2) was added to terminate the reaction. The fluorescence intensity corresponding to the released 7-amino-4-methyl-coumarin was measured at 460 nm with excitation at 380 nm (FP-6300, JASCO Corporation, Tokyo, Japan). After pepsin treatment (see below), the acidic pH was neutralized by adding 1.6 volume of 0.2 M Tris-HCl (pH 9.0) and activity measurement was performed.

2.4. Sodium dodecyl sulphate-polyacrylamide gel electrophoresis (SDS-PAGE) and western blotting analysis

Two micrograms of proteins in the EV fractions, prepared as described above, were separated using SDS-PAGE on SuperSep HG, 5–20% gradient gels (FUJIFILM Wako Pure Chemical Corporation, Osaka, Japan). Protein bands were visualized using silver staining (2D-Silver Stain Reagent II, Cosmo Bio, Tokyo, Japan). To detect specific proteins in the salivary EVs, protein bands were transferred onto polyvinylidene difluoride (PVDF) membranes (BSP0161, Pall Corporation, MA, USA) using a wet transfer method (1703930JA, Bio-Rad Laboratories, Inc., Hercules, CA, USA). Nonspecific binding sites were blocked by incubating the membranes in 100 mM Tris-HCl (pH 7.4) and 150 mM NaCl with 5% skim milk and 1% Tween 20. The membranes were then incubated overnight at 4 °C with rabbit anti-mucin 5B (1:1,000, H-300, Santa Cruz Biotechnology, Inc., Dallas, TX, USA), goat *anti*-IgA (1:1,000, A80-102A, Bethyl Laboratories, Montgomery, TX, USA), goat *anti*-DPP

IV (1:1,000, AF1180, R&D Systems, Inc., Minneapolis, MN, USA), rabbit anti-CD9 (1:1,000, EXOAB-CD9A-1, System Biosciences, Mountain View, CA, USA), goat *anti*-Alix (1:1,000, Q-19, Santa Cruz Biotechnology, Inc., Dallas, TX, USA), or mouse *anti*-TSG101 (1:1,000, 4A10, Abcam, Cambridge, MA, USA) primary antibodies, followed by incubation with horseradish peroxidase-labeled secondary antibodies (1:5,000; anti-goat antibodies, 811620, Thermo Fisher Scientific; anti-rabbit antibodies, W4011, and anti-mouse antibodies, W4021, Promega Corporation, WI, USA). The protein bands were visualized using a LAS-4000 mini luminescent image analyzer (GE Healthcare Bio-Science Corp., Piscataway, NJ, USA) and the ECL prime western blotting detection kit (GE Healthcare). Immunoreactive bands were quantified using the Image J software (National Institutes of Health, Bethesda, MD, USA).

2.5. Transmission electron microscopy (TEM)

TEM analysis was performed as described previously, with minor modifications [6]. Briefly, the concentrated EV fractions, prepared as described above, were mixed with 25% glutaraldehyde in phosphate buffer (pH 7.2) in a ratio of 9:1 and then applied to collodion-coated 200-mesh copper grids. The grids were stained with 2% uranyl acetate (pH 7) and embedded with 2% methylcellulose/0.4% uranyl acetate (pH 4). After drying, the grids were examined using TEM (TEM-1010; JEOL, Tokyo, Japan).

2.6. Immunoelectron microscopy

The samples were mixed with 4% paraformaldehyde in phosphate buffer (pH 7.2) in a 1:1 ratio and then applied to 200-mesh Formvar carbon-coated nickel grids. After blocking with 5% normal donkey serum and washing with PBS, the grids were incubated with either goat anti-human DPP IV (1:100, AF1180, R&D Systems, Inc., Minneapolis, MN, USA) and mouse *anti*-Alix (1:100, 3C4, Abnova Corp., Taipei City, Taiwan) or goat *anti*-DPP IV (1:100, R&D Systems, Inc., Minneapolis, MN, USA) and mouse *anti*-TSG101 (1:100, 4A10, Abcam, Cambridge, MA, USA) primary antibodies overnight at 4 °C. The grids were then washed with PBS and exposed to 6 nm colloidal gold-conjugated donkey anti-mouse IgG (705-195-147, Jackson Immunoresearch, West Groove, PA, USA) and 12 nm colloidal gold-conjugated donkey anti-goat IgG (715-195-150, Jackson Immunoresearch) for 1 h at room temperature (20–25 °C). After washing, the grids were re-fixed in 1% glutaraldehyde-PBS, stained with 2% uranyl acetate (pH 7), and washed with distilled water. After drying, the grids were examined using TEM (JEM-1011, JEOL, Tokyo, Japan).

2.7. Dynamic light scattering (DLS) studies

The size distribution profile of salivary EVs was determined via DLS, based on the laser diffraction method, using a Zetasizer Nano-ZS90 instrument (Malvern Instruments, Worcestershire, UK). EV fractions containing 10 μg protein/mL were analyzed at a constant temperature (25 °C); the buffer viscosity was 0.8872 cP, and the buffer refractive index, particle absorption, and particle refractive index were set to 1.33 η, 0.010, and 1.59 η, respectively. The DLS signal intensity was transformed to volume distribution [volume (%)], assuming the EVs were spherical in shape. Data sets were acquired and analyzed using the proprietary Malvern software.

2.8. Determination of the stability of salivary EVs under simulated gastrointestinal conditions

To analyze the stability of EVs under oral and intestinal conditions, EV fractions were incubated at 37 °C for up to 3 h at pH 7.4 (neutral condition) or at pH 3.0 (acidic condition). Additionally, to simulate the gastric fluids, EV fractions (0.1 mg/mL) were treated with pepsin (0.03–3.0 mg/mL) and incubated at pH 3.0 and 37 °C for 3 h. The pH was then adjusted to around 7 using 1.6 volume of 0.2 M Tris-HCl buffer (pH 9.0). To simulate the intestinal fluids, the indicated concentrations of pancreatin (0.01–1.0 mg/mL) were added to the EV fractions (0.1 mg/mL) and the mixtures were incubated at pH 7.4 and 37 °C for 1 h. Finally, protease inhibitor cocktail dissolved in PBS was added to each fraction and incubated for 15 min at room temperature to stop the enzymatic reactions. Silver staining, western blotting, DPP IV activity measurement, TEM, and DLS were used to determine the effect of the simulated gastrointestinal conditions on the salivary EV fractions.

2.9. Detergent treatment of salivary EVs

To evaluate the detergent-like effect of the bile salts present in intestinal fluids on salivary EV fractions, the indicated concentrations of sodium cholate (0.1–1.0%) were added to the EV fractions (0.1 mg/mL) and the mixtures were incubated at 25 °C and pH 7.4 for 30 min. The fractions were then subjected to ultracentrifugation at 100,000×*g* for 2 h at 10 °C (himac CS150NX; S100AT0115 rotor; Koki Holdings Co., Ltd. Tokyo, Japan), and the supernatants were collected. The pellets were suspended in PBS and subjected to DLS or electron microscopy analyses. Additionally, for DPP IV activity measurements, the pellets were washed in 100 μL PBS by ultracentrifugation at 100,000×*g* for 1 h at 10 °C to remove sodium cholate that affects DPP IV activity. Each pellet was then homogeneously suspended in 1% NP-40 in PBS. DPP IV activity was marginally affected by the addition of 1% NP-40 ($111.2 \pm 12\%$, $n = 5$). For Western blot analysis, protease inhibitor cocktail in PBS was added to the pellets and the samples were incubated for 15 min at room temperature prior to denaturation by sample buffer.

2.10. Digestive enzymes and detergent treatment of salivary EVs

The milieu of the intestine was also simulated using a physiological concentration of sodium cholate (0.1% or 0.4%) and the indicated concentration of pancreatin (0.01–1.0 mg/mL), which were added to the EV fractions (0.1 mg/mL). The mixtures were incubated at pH 7.4 and 37 °C for 1 h. After enzymatic treatment, protease inhibitor cocktail dissolved in PBS was added and the fractions were incubated for 15 min at room temperature prior to silver staining, western blotting, and DLS analysis.

2.11. Sequential treatment of salivary EVs

EV fractions (0.1 mg/mL) were first treated with the indicated concentration of pepsin (0.03–0.0 mg/mL) at 37 °C and pH 3.0 for 3 h. Next, the pH was adjusted to around 7 using a 1.6 volume of 0.2 M Tris-HCl buffer (pH 9.0), and the resulting EV fractions were treated with the indicated concentration of pancreatin (0.01–1.0 mg/mL) and a physiological concentration of sodium cholate (0.1%) at 37 °C for 1 h. The concentration of the two enzymes used in combination for this treatment was categorized into low (0.03 mg/mL pepsin and 0.01 mg/mL pancreatin), medium (0.3 mg/mL pepsin and 0.1 mg/mL pancreatin), or high (3.0 mg/mL pepsin and 1.0 mg/mL pancreatin). After these enzymatic treatments, protease inhibitor cocktail dissolved in PBS was added to the EV fractions and incubated for 15 min at room temperature prior to silver staining, western blotting, and DLS analysis.

2.12. Statistical analysis

All data are representative of at least three independent experiments and shown as the mean ± standard deviation. Statistical analysis was performed using the Student's t-test and one-way ANOVA followed by Tukey-Kramer post-hoc analysis, and $P < 0.05$ was considered to indicate statistically significant results.

3. Results

3.1. Identification and preparation of human salivary extracellular vesicles

Fig. A.1 shows the characteristics of human salivary EV fractions employed in this study. EV fractions from WS collected from a single healthy volunteer were purified using gel filtration column chromatography as described in "Materials and Methods". As shown in Fig. A.1A, the salivary EV fractions that eluted in a single peak after the void volume of Sephacryl S-500 column were monitored for DPP IV activity. Most of the fractions that contained contaminating proteins and failed to show DPP IV activity were removed; only the fractions 31–39 exhibited DPP IV activity and were pooled, concentrated, and used for further studies. Fig. A.1B shows the Western blot analysis of the collected EV fractions. DPP IV, Alix and TSG101, which are generally accepted cytosolic proteins retained in EVs, and CD9, a typical transmembrane protein of EVs [1], were co-eluted, confirming that the pooled fraction contained EVs. Furthermore, mucin 5B and IgA, which are salivary proteins, were also co-eluted suggesting their association with these EVs. Therefore, we evaluated the stability and integrity of this salivary EV fraction by monitoring its DPP IV activity and the presence of these six aforementioned proteins. Morphological analyses through TEM indicated that the fractions contained distinctive particles with an average diameter of 40 nm [6] and contained DPP IV together with Alix and/or TSG101 (Fig. A.1C). The total amount of protein in the EV fractions obtained from 40 mL of WS from a donor was 1.17 ± 0.67 mg (n = 30). The total DPP IV activity in the EV fractions was 8.83 ± 6.9

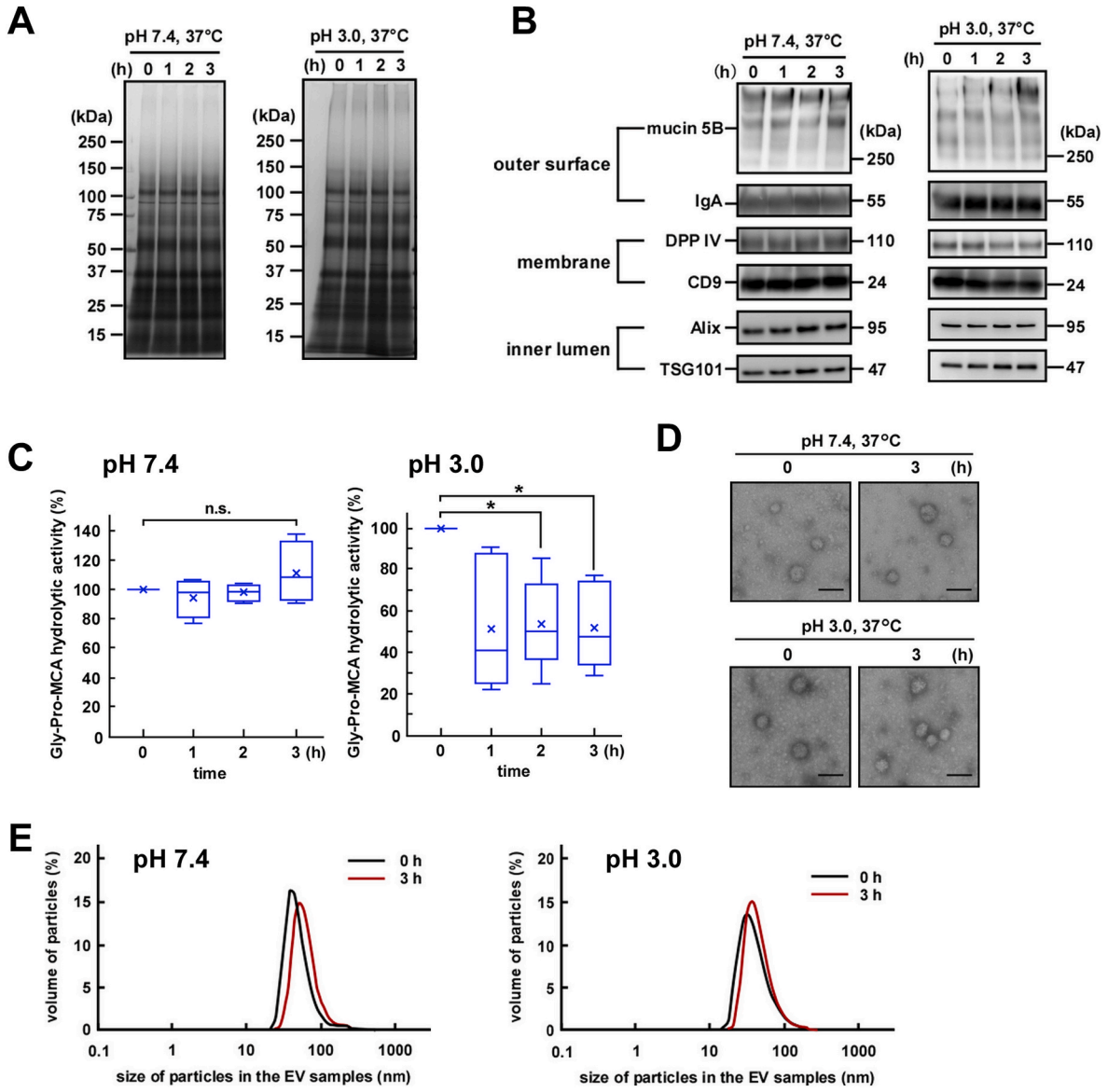

Fig. 1. Stability of salivary extracellular vesicles (EVs) incubated at 37 °C under neutral or acidic conditions. Salivary EV fractions were incubated at 37 °C at either pH 7.4 or pH 3.0 over the indicated duration. (A) Two micrograms of proteins from each EV fraction were subjected to SDS-PAGE and visualized via silver staining (donor A). (B) Western blot analysis of the proteins located on the outer surface (mucin 5B and IgA), membrane (DPP IV and CD9), and inner lumen (Alix and TSG101) of the salivary EVs, (donor A). The EV fractions were incubated at either pH 7.4 or pH 3.0. Two micrograms of proteins from each treated EV fraction were subjected to SDS-PAGE, transferred onto PVDF membranes, and immunoblotted with antibodies. (C) Changes in the DPP IV activity in the salivary EV fractions. The DPP IV activity in fresh or treated EV fractions is represented by box plots referring to four (pH 7.4) or six (pH 3.0) experiments with triplicates. The mean is denoted as x. *, $p < 0.05$, n. s., not significant. (D) Morphological analyses of the salivary EV fractions visualized under an electron microscope (donor A). Zero hours represents fresh EV fractions. Scale bar, 100 nm. The morphology of EVs from other donors is shown in Fig. A.2C. (E) Particle sizes of the salivary EVs analyzed via DLS measurements conducted in triplicates. A typical result is shown (donor A).

nmol/min (n = 30), and the specific activity of the enzyme was 8.94 ± 7.1 nmol/min/mg protein. The EV fractions contained 1.55 ± 0.83% of the total protein of WS and 30.6 ± 15% of the total DPP IV activity of WS (n = 30). A decrease in recovery of the total activity was observed during filtration and concentration. This may be because of the absorbance to filtration devices. DPP IV activity was measured in each step during preparation and rarely detectable in other fractions including the filtrate. Therefore, we used DPP IV as one of the transmembrane protein markers associated with salivary EVs.

3.2. Stability of EVs under acidic and neutral conditions

Since EVs encounter acidic conditions in the stomach after being secreted into the saliva and passing through the esophagus, we first examined the effect of acidic conditions on the stability and integrity of EV fractions purified from WS. Under acidic conditions (pH 3.0), EV fractions were stable after 3 h of incubation and overall protein degradation was not detectable (Fig. 1A). Similarly, no protein degradation was detected upon incubation of EV fractions under neutral conditions (pH 7.4).

Next, we examined the degradation of specific proteins located on the EV membrane (DPP IV and CD9), in the inner lumen (Alix and TSG101), and on the outer surface of the EV membrane (mucin 5B and IgA) during incubation under neutral or acidic conditions (Fig. 1B). As expected, under neutral conditions, a decrease in the tested protein levels was not observed for up to 3 h. Additionally, under acidic conditions, densitometric analyses showed no significant decrease in the protein levels, although levels of CD9 and Alix tended to decrease after 3 h of exposure to the acidic condition (Fig. A.2A). These results suggest that the overall primary structures of EV-associated proteins remain intact under the acidic condition, mimicking the pH of the stomach.

We then measured the EV-associated DPP IV activity (Fig. 1C). Under neutral conditions, no decrease in the enzymatic activity was observed for up to 3 h. However, exposure to acidic conditions led to a statistically significant decrease in the DPP IV activity after 2–3 h. On the other hand, degradation of DPP IV was not observed, suggesting the partial denaturation of the enzyme upon prolonged exposure. As a control, we also measured the activity of rhDPP IV (the soluble form DPP IV) and found little difference compared to that of EV-associated DPP IV (membrane-bound DPP IV) (Fig. A.2B).

The morphological integrity of salivary EV fractions was also monitored via TEM. As shown in Fig. 1D, fresh salivary EV fractions contained distinctive particles with diameters of 30–70 nm. Exposure to either neutral or acidic conditions for 3 h did not cause any apparent changes in the particle diameter or morphology (Fig. 1D and Fig. A.2C). Similarly, DLS studies revealed no significant difference in the particle size between the EVs incubated at pH 7.4 and 3.0 (Fig. 1E and Fig. A.2D). Taken together, we concluded that under acidic conditions, salivary EV fractions maintained their overall functional stability and morphological integrity for at least up to 3 h, which is sufficient for a consumed diet to pass through the stomach.

3.3. Effects of gastrointestinal enzymes on the stability of EVs

After entering the gastrointestinal tract, salivary EVs encounter pepsin in the stomach and pancreatic enzymes. Since proteases might affect the function and morphology of the membranous structure of EVs via degradation of their protein components, we next examined the effects of the proteases on the stability and integrity of the EV fractions. Considering the physiological concentrations of the enzymes, we used a concentration range of 0.03–3.0 mg/mL for pepsin and 0.01–1.0 mg/mL for pancreatin that contains alpha-amylase, trypsin, lipase, and phospholipase A_2 (PLA_2). In the time-course study, the changes observed in the levels of the protein components of EVs reached a plateau after 2-h treatment with pepsin and 30-min treatment with pancreatin (Fig. A.3A). Therefore, we examined degradation of these protein components upon treatment with pepsin for 3 h or pancreatin for 1 h. Regarding the effects of pepsin on the protein content of the EV fractions, only the highest concentration (3 mg/mL) of pepsin induced a slight disappearance of the ~120 kDa component, while pancreatin had a minor effect on the overall protein components of the EV fractions up to 1 mg/mL (Fig. 2A).

Next, the degradation of the protein components was further characterized using western blotting. Depending on the enzyme concentration used for treatment, pepsin degraded mucin 5B and CD9 by statistically significant amounts (Fig. 2B, dose response and Fig. A.3B, dose response). Time course experiments showed that rapid degradation of mucin 5B was observed within 5 min (Fig. 2B, time course and Fig. A.3B, time course) of treatment, while degradation of CD9 was rather slow. These results suggested that pepsin had access to the outside of the EVs and was able to degrade mucin 5B that remained exposed outside. As in the case of pepsin, pancreatin-mediated degradation of mucin 5B occurred rapidly and that of CD9 was slow. Since pancreatin used in this study was a mixture of at least four enzymes, including alpha-amylase, trypsin, lipase, and PLA_2, it is possible that protease was able to penetrate into the lumen via perturbation of the membrane structure of EVs, presumably mediated by PLA_2, and caused the degradation of Alix. In addition, DPP IV and IgA were not degraded by both the enzymes (Fig. 2B and Fig. A.3B). However, treatment of salivary EV fractions with pepsin caused a decrease in the enzymatic activity of DPP IV (Fig. 2C, left and Fig. A.3C, left). Considering DPP IV activity was decreased only under acidic conditions (Fig. 1C), it was likely that the decrease was not because of DPP IV degradation. Although rhDPP IV activity showed the same tendency by pepsin treatment, it is likely that rhDPP IV was degraded by the enzyme. Therefore, the degradative susceptibility of a membrane-bound DPP IV in gastric environment might be different from that of a soluble form. (Fig. A.3D). In contrast, a slight increase in DPP IV activity was observed after the treatment of the salivary EV fractions with pancreatin (Fig. 2C, right and Fig. A.3C, right). To determine whether pancreatin affects DPP IV directly, we digested rhDPP IV with pancreatin and found a slight but statistically significant increase in DPP IV activity (Fig. A.3D). Nevertheless, the mechanism behind such an increase in DPP IV activity remains unknown. Thus, it was apparent that unlike CD9, EV-associated DPP IV was resistant to both the enzymes despite its exposure to the extracellular milieu.

The morphological analyses using electron microscopy showed that the EVs retained their morphological integrity even after the protease treatment (Fig. 2D and Fig. A.3E). In addition, particle size analyses by DLS (Fig. 2E and Fig. A.3F) showed that EVs retained similar diameters irrespective of the protease-mediated degradation of certain membrane protein components. It is thus conceivable that the salivary EVs are rather stable and may maintain morphological integrity during their retention in the gastrointestinal tract, if detergent activity of bile acids is not considered (see below). However, it may be possible that proteases in the tract induce instability in the EV particles via the degradation of exposed membrane proteins to release certain luminal components, such as Alix.

3.4. Effect of sodium cholate on the stability of EVs

In the duodenum and small intestine, salivary EVs are mixed with bile acids in addition to pancreatic enzymes. Bile acids contain cholic acid as a major component that acts as a detergent. We next examined the solubility of the EV-associated proteins after treatment of the EV fractions with sodium cholate, centrifugation, and separation of the supernatant fraction from the precipitated fraction, followed by analysis using SDS-PAGE. Because the critical micelle concentration (CMC) of sodium cholate is 14 mmol/L (0.56%), we used sodium cholate at 0.1% (minimum physiological concentration), 0.6% (CMC), and 1.0% (locally high concentration in the intestine). Mucin 5B and IgA were released into the supernatant fraction without sodium cholate, indicating that

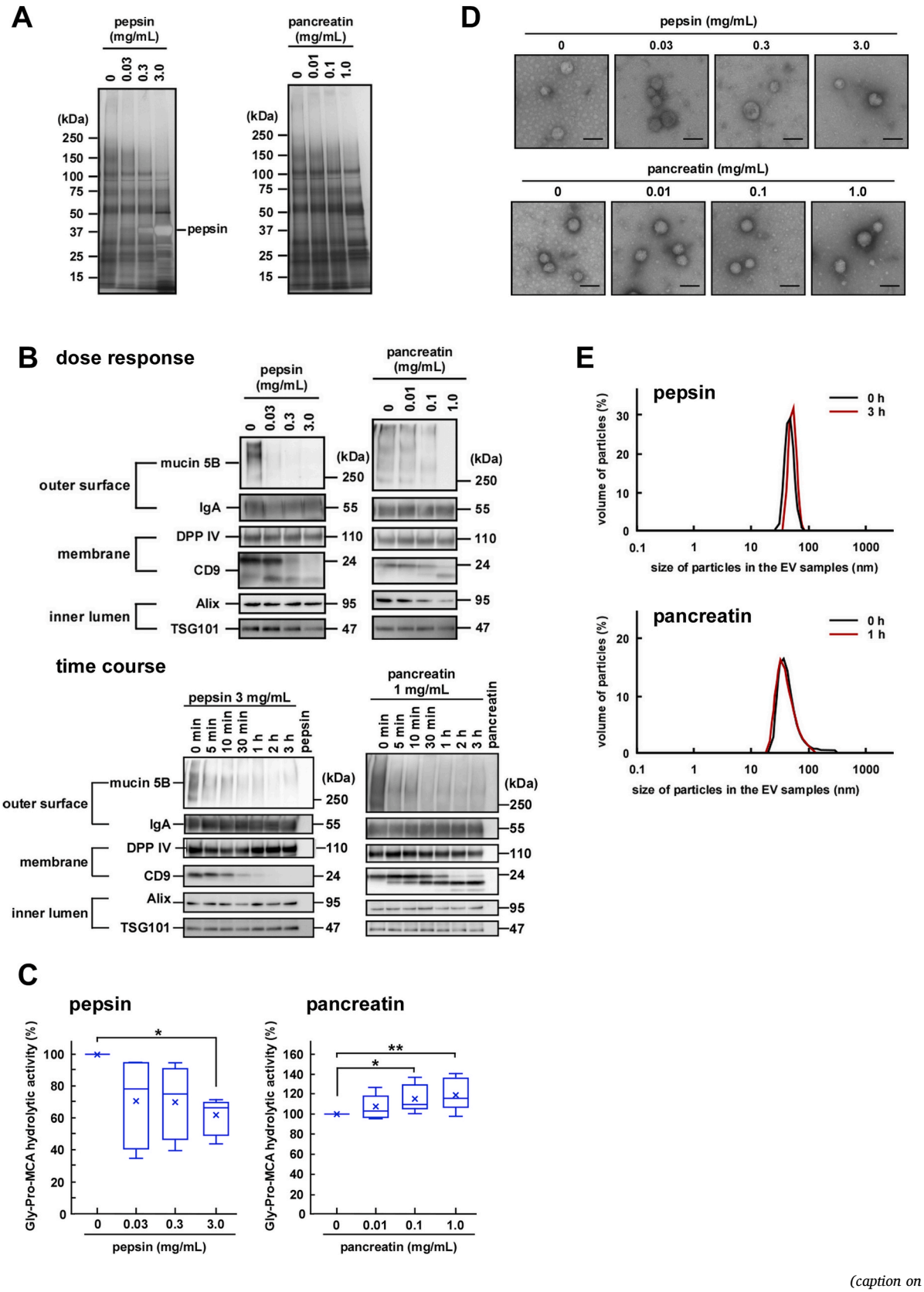

(caption on next page)

Fig. 2. Stability of salivary extracellular vesicles (EVs) in the presence of gastrointestinal enzymes. The indicated concentrations of pepsin or pancreatin were added to the EV fractions and the mixtures were incubated at pH 3.0, 37 °C for 3 h or at pH 7.4, 37 °C for 1 h, respectively. (A) Two micrograms of proteins from each treated EV fraction were subjected to SDS-PAGE, and visualized vis silver staining after either pepsin or pancreatin digestion (donor A). (B) Western blot analysis of the proteins located on the outer surface (mucin 5B and IgA), membrane (DPP IV and CD9), and inner lumen (Alix and TSG101) of salivary EVs was also performed (donor A). Two micrograms of proteins from each treated EV fraction were subjected to SDS-PAGE, transferred onto PVDF membranes, and immunoblotted with antibodies. For the time-course study, pepsin (3 mg/mL) or pancreatin (1 mg/mL) was added to the EV fractions and the mixtures were incubated at pH 3.0, 37 °C or at pH 7.4, 37 °C, respectively, for the indicated times. (C) Changes in the DPP IV activity in the salivary EV fractions. The DPP IV activity in fresh or treated EV fractions is represented by box plots referring to six (pepsin) or ten (pancreatin) experiments conducted in triplicates. The mean is denoted as x. *, $p < 0.05$, **, $p < 0.01$. (D) Morphological analyses of the salivary EV fractions. The EV fractions were incubated with pepsin (donor D) or pancreatin (donor A) and transmission electron microscopy analysis was performed. Scale bars, 100 nm. The morphology of the EVs from other donors is shown in Fig. A 3E. (E) Particle size of the salivary EVs. The EV fractions were treated with 3 mg/mL pepsin for 3 h or 1 mg/mL pancreatin for 1 h and the particle size was analyzed using DLS (measurements conducted in triplicates). A typical result is shown (donor H for pepsin, and donor A for pancreatin).

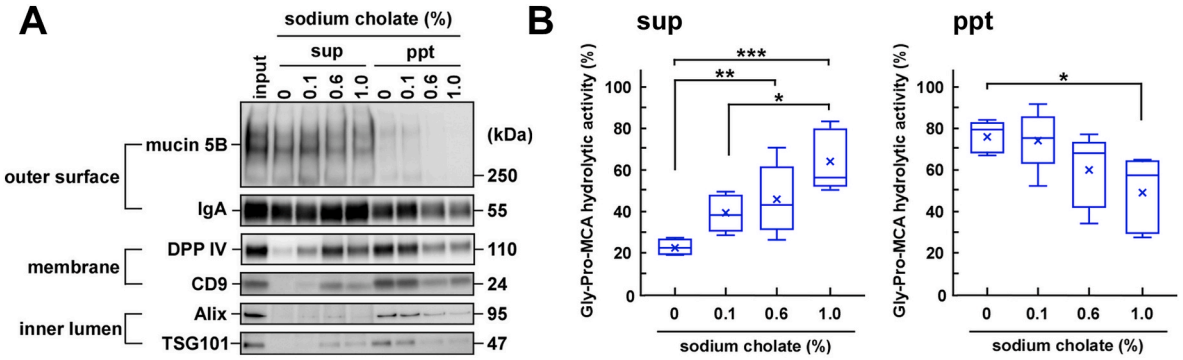

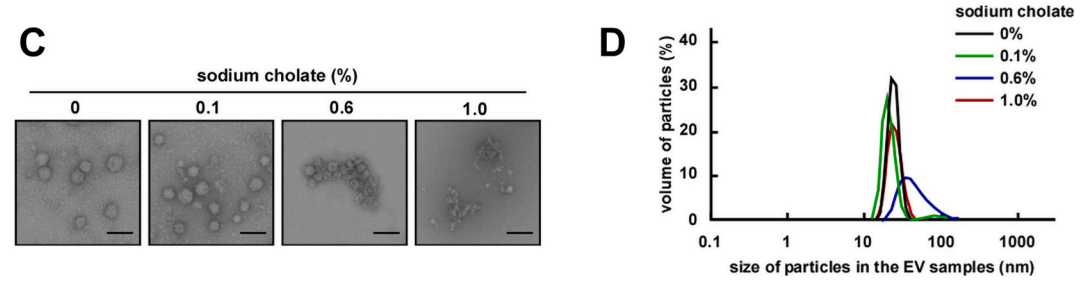

Fig. 3. Stability of salivary extracellular vesicles (EVs) in the presence of sodium cholate. The indicated concentration of sodium cholate was added to the EV fractions and the mixtures were allowed to stand for 30 min at 25 °C. Then, the fractions were ultracentrifuged at 100,000×*g* for 2 h at 10 °C and the resulting supernatants (sup) and precipitates (ppt) were used for further analysis. Input refers to the EV fractions that were not treated with sodium cholate or subjected to ultracentrifugation. (A) Western blot analysis of the proteins located on the outer surface (mucin 5B and IgA), membrane (DPP IV and CD9), and inner lumen (Alix and TSG101) of salivary EVs (donor A). Two micrograms of proteins from the treated EV fractions were subjected to SDS-PAGE, transferred onto PVDF membranes, and immunoblotted with antibodies. (B) Changes in the DPP IV activity of salivary EVs. The DPP IV activity in the untreated or treated EV fractions was measured in triplicates and is represented as box plots of five independent experiments. The mean is denoted as x. *, $p < 0.05$; **, $p < 0.01$; ***, $p < 0.001$. The DPP IV activity in the untreated EV fraction before ultracentrifugation (input) was assumed to be 100%. (C) Morphological analyses of the salivary EV fractions visualized under an electron microscope (donor A). Scale bar, 100 nm. The morphology of EVs from other donors is shown in Fig. A.4C. (D) Particle size of the salivary EVs. The particle size was analyzed using DLS measurements carried out in triplicates. A typical result is shown (donor A).

separation occurred during ultracentrifugation due to the weak association of these two proteins with the EVs (Fig. 3A and Fig. A.4A). Mucin 5B is associated with the outside of the EV membrane and is easily released from the particle during storage [9]. Additionally, looking closely at the gels, it seems likely that a decrease in the protein concentration of the precipitated fractions and an increase in that of the supernatant fractions in a detergent-concentration-dependent manner suggested a detergent-mediated solubilization of the membrane structure of EVs. Densitometric analyses also supported the notion that treatment of the EV fractions with the detergent caused the transfer of the proteins from the precipitated fraction (ppt) to the supernatant fraction (sup) (Fig. A.4A). The distribution of the DPP IV activity also showed the same tendency (Fig. 3B), confirming the solubilization of the membranes. Of note, the activity of EV-associated (membrane-bound) DPP IV and rhDPP IV (soluble form) was retained in the presence of sodium cholate (Fig. A.4B). However, the transfer of component proteins from ppt to sup could not be quantified; this was also observed in our previous study, presumably owing to experimental challenges, including adsorption of the proteins to the experimental tubes and/or protein degradation by some proteolytic enzymes present in the purified EV fractions [9].

To determine the effect of detergent treatment on EV membrane integrity, electron microscopy and DLS analyses were further performed (Fig. 3C, D, Fig. A.4C [morphology of other donors] and Fig. A.4D). In the presence of 0.1% sodium cholate, the overall particle morphology and average particle size remained intact. However, at higher concentrations, aggregated and/or fragmented membranes were seen. When the aggregated form was dominant (i.e., 0.6% sodium cholate), the average particle size was increased. Conversely, in the presence of 1.0% cholate, the particle size was reversed, presumably owing to fragmentation. These results suggested that in the presence of sodium cholate, the membrane of EVs was perturbed and/or fragmented, leading to the solubilization of the membrane proteins (DPP IV and CD9) and the consequent transfer from the precipitate to the supernatant. Moreover,

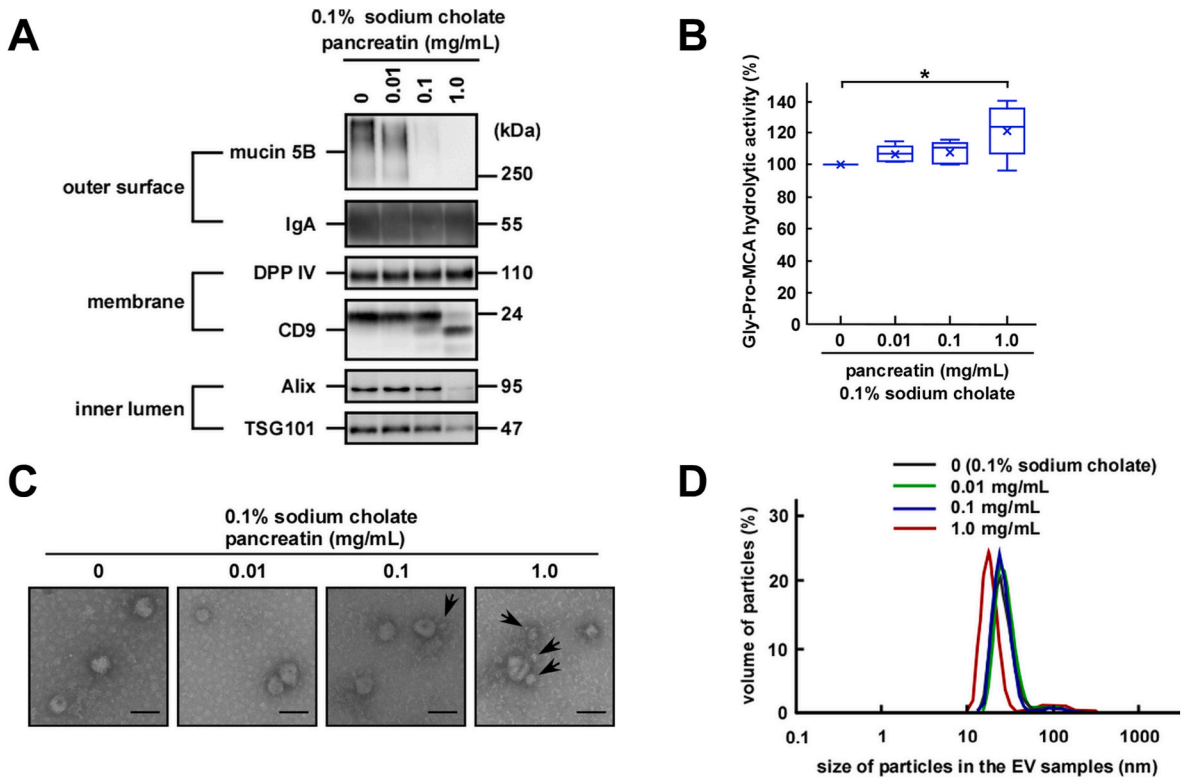

Fig. 4. Stability of salivary extracellular vesicles (EVs) in the presence of sodium cholate and pancreatin. The indicated concentration of pancreatin was added to the EV fractions in the presence of 0.1% of sodium cholate and the mixtures were incubated at pH 7.4, 37 °C for 1 h. (A) Western blot analysis of the proteins located on the outer surface (mucin 5B and IgA), membrane (DPP IV and CD9), and inner lumen (Alix and TSG101) of salivary EVs (donor A). Two micrograms of proteins from each treated EV fraction were subjected to SDS-PAGE, transferred onto PVDF membranes, and immunoblotted with antibodies. (B) Changes in the DPP IV activity in salivary EV fractions. The DPP IV activity in fresh or treated EV fractions was measured in triplicates and is represented as box plots of five independent experiments. The mean is denoted as x. *, $p < 0.05$. (C) Morphological analyses of the salivary EV fractions visualized under an electron microscope (donor A). Black arrows point to EVs with smaller sizes. Scale bar, 100 nm. The morphology of EVs from other donors is shown in Fig. A.5B. (D) Particle size of salivary EVs. The particle size was analyzed using DLS measurements conducted in triplicates. A typical result is shown (donor K).

Alix and TSG101 were released from the inner lumen of the EVs into the supernatant. Since physiological concentrations of cholic acid in the intestine were estimated to be generally in the range of 0.1%–0.4% [17, 18], we also examined the effect of 0.4% cholate and found no additional effects (Fig. A.4E). Thus, it is speculated that salivary EVs are destabilized in the presence of higher concentrations of bile acids, releasing their luminal and membranous contents into the intestine.

Since bile acids and pancreatin are co-localized in the intestine, we next examined the effects of this enzyme in the presence of a physiological concentration (0.1%) of sodium cholate on the EV fractions (Fig. 4). In line with the results obtained with pancreatin alone, treatment with pancreatin in the presence of 0.1% sodium cholate caused statistically significant degradation of mucin 5B (the surface-associated protein) and CD9 (the transmembrane protein) (Fig. 4A and Fig. A.5A). In addition, the disappearance of Alix and TSG101 (inner lumen-associated proteins) was observed. However, DPP IV was not degraded and its enzymatic activity was entirely retained (Fig. 4A and B). The activity was substantially increased, presumably only by the pancreatin treatment, as shown previously in Fig. 2C (Fig. 4B); of note, the activity of DPP IV was not affected when incubated with 0.1% sodium cholate alone [98.2 ± 14% of control in PBS (pH 7.4) for 1 h at 37 °C].

Morphological analyses using electron microscopy revealed that the EVs remained intact in the presence of up to 0.1 mg/mL of pancreatin even in the presence of 0.1% sodium cholate (Fig. 4C and Fig. A.5B). Notably, EVs with a smaller particle size were observed when treated with a higher concentration of pancreatin as highlighted with black arrows in Fig. 4C, although large particles were also observed. In addition, in the DLS analyses, approximately 25% decrease in the average size of the EVs was observed when treated with 1.0 mg/mL of pancreatin in the presence of 0.1% sodium cholate (Fig. 4D and Fig. A.5C). In the absence of sodium cholate, a decrease in the average particle size was not observed (Fig. 2E). Taken together, sodium cholate facilitated the fragmentation and destabilization of EV membrane, thereby allowing pancreatin to access the membrane and luminal contents more easily. We also examined the effect of 0.4% cholate and pancreatin, and no additional effect was observed (Fig. A.5D).

3.5. *Effects of sequential treatments on the stability of EVs*

To further simulate the conditions of the gastrointestinal tract, the EV fractions were first treated with pepsin under acidic conditions followed by a combined treatment with pancreatin and sodium cholate. Because the concentration of enzymes in the gastrointestinal tract is increased at fasting and decreased at refeeding, we set the combination of the enzyme as low (0.03 mg/mL pepsin and 0.01 mg/mL pancreatin), medium (0.3 mg/mL pepsin and 0.1 mg/mL pancreatin) or high (3.0 mg/mL pepsin and 1 mg/mL pancreatin). As shown in Fig. 5A and Fig. A.6A, the sequential treatment with low concentrations of pepsin and pancreatin caused almost the complete degradation of mucin 5B. However, DPP IV and IgA remained intact even at high concentrations of pepsin and pancreatin. In contrast, CD9, Alix, and TSG101 were degraded at pancreatin concentrations lower than those of the combined treatment with pancreatin and sodium cholate as shown in Fig. 4A. These results suggested that the prior treatment with pepsin under acidic conditions might have primed the EVs to be more sensitive to the subsequent attack by pancreatin. DPP IV activity was almost the same as

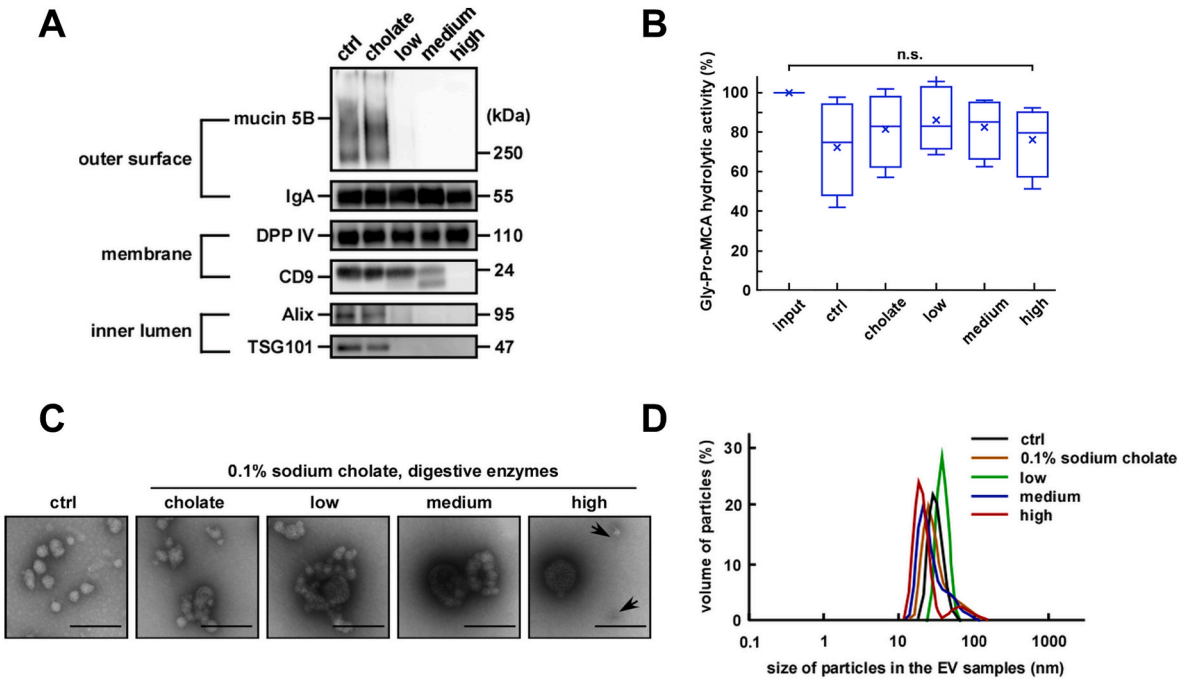

Fig. 5. Stability of salivary extracellular vesicles (EVs) after sequential treatment. After pepsin treatment under acidic conditions (0.03–3.0 mg/mL, pH 3.0, 37 °C for 3 h) the pH was neutralized. Then sodium cholate (0.1%) and pancreatin (0.01–1 mg/mL) were added to the EV fractions and the mixtures were incubated at 37 °C for 1 h. The different combinations of enzyme concentrations used were low (0.03 mg/mL pepsin and 0.01 mg/mL pancreatin), medium (0.3 mg/mL pepsin and 0.1 mg/mL pancreatin) and high (3.0 mg/mL pepsin and 1.0 mg/mL pancreatin). (A) Western blot analysis of the proteins located on the outer surface (mucin 5B and IgA), membrane (DPP IV and CD9), and inner lumen (Alix and TSG101) of salivary EVs (donor A). Two micrograms of proteins from each treated EV fraction were subjected to SDS-PAGE, transferred onto PVDF membranes, and immunoblotted with antibodies. (B) Changes in the DPP IV activity in the salivary EV fractions. The DPP IV activity in fresh or treated EV fractions was measured in triplicates and is represented as box plots of five independent experiments. The mean is denoted as x. n. s., not significant. The mean is denoted as x. Input indicates fresh and untreated EV fractions, and control (ctrl) indicates EV fractions only subjected to changes in the pH (from pH 3 to pH 7). (C) Morphological analyses of the salivary EV fractions visualized under an electron microscopy (donor A). Black arrows highlight smaller EVs. Scale bar, 100 nm. The morphology of EVs from other donors is shown in Fig. A.6B. (D) Particle size of salivary EVs. The particle size was analyzed using the DLS measurements conducted in triplicates. A typical result is shown (donor A).

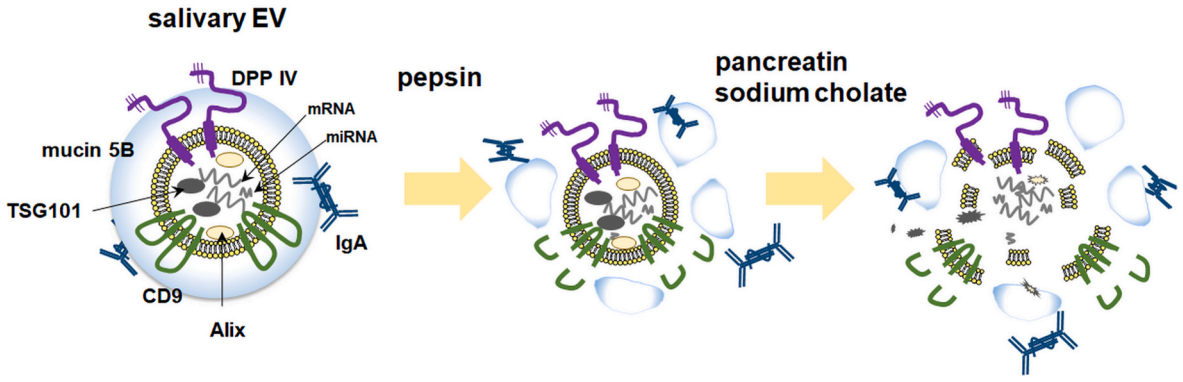

Fig. 6. A schematic model of the components of salivary extracellular vesicles (EVs) and their stability under gastrointestinal conditions.

that of the EV fractions treated with only pepsin under acidic conditions, as shown previously in Fig. 2C, suggesting that the sequential treatment had no additional effect on DPPIV activity (Fig. 5B).

Morphological analyses using electron microscopy showed that the sequential treatment induced drastic changes in the EV particle size and morphology (Fig. 5C and Fig. A.6B). After combined treatment with low or medium concentrations of pepsin and pancreatin, large, fused, or aggregated EV forms were observed. Conversely, treatment with high concentrations of the proteases caused the apparent fragmentation of the particles similar to that observed for the EV fractions treated with 1.0 mg/mL of pancreatin in the presence of 0.1% sodium cholate. In DLS analyses (Fig. 5D and Fig. A.6C), an increase in the average particle size was observed after treatment with low concentrations of proteases, presumably owing to particle fusion and aggregation, as observed in Fig. 5C. Considering the luminal proteins (Alix and TSG101) were not detected using western blotting, it is most likely that the EV fractions became unstable and leaky under simulated gastrointestinal tract conditions.

4. Discussion

In this study, the morphological stability and membrane integrity of human salivary EVs were characterized to determine their fate in the gastrointestinal tract (Fig. 6). Several EV membrane surface-associated

proteins were degraded in the presence of pepsin, suggesting that pepsin could access and degrade both mucin 5B located on the outer surface of the EVs and the transmembrane protein CD9. Sequential treatments with pepsin and pancreatin/sodium cholate made the EVs more susceptible to membrane perturbation and fragmentation leading to the release and solubilization of their membrane and luminal protein contents. Taken together, these results indicate that salivary EVs may undergo destabilization and fragmentation in the intestine to release their contents.

Under acidic conditions in the presence of pepsin, simulating the milieu of the stomach, several EV membrane surface-associated proteins are degraded. Salivary EVs may subsequently undergo destabilization and fragmentation under the intestinal conditions to release their contents, whereas DPP IV and IgA remain intact.

We pursued DPP IV as one of the markers of salivary EVs. Although a decrease in the DPP IV activity was observed under acidic conditions, no significant degradation occurred even upon sequential treatment with pepsin and pancreatin/sodium cholate. Thus, the decrease of the DPP IV activity under acidic conditions may be because of the conformational change of its catalytic site and was reversible when neutralized (Fig. 5B). On the other hand, the increase of the DPP IV activity by pancreatin (with or without sodium cholate) might be because of the exposure of its active site via the degradation of other proteins such as mucins around DPP IV. Therefore, our results suggest DPP IV as a valuable indicator of the stability of EV membrane structures.

It is thus plausible that DPP IV activity in salivary EVs is largely retained during transit through the gastrointestinal tract. It was apparent that unlike CD9, DPP IV was resistant to both the enzymes despite its exposure to the extracellular milieu. DPP IV is highly glycosylated (nine glycosylated sites) [10], which might have protected it from access by the proteases, while CD9 has only two glycosylated sites. Moreover, DPP IV is preferentially localized to lipid raft domains rich in sphingolipids and cholesterol [19]. Glycosylation and/or localization sites of the membrane proteins in EVs might be critical for the accessibility and/or resistance to proteases attacking from the outside. It is also possible that proteins such as IgA associated with the outer surface of EVs protect this enzyme from protease catalysis [20].

DPP IV is also expressed on the brush-border membranes of the small intestine [10]. It is also demonstrated that intestinal epithelial cells secrete exosome-like vesicles containing DPP IV [21]. Gastrointestinal proteases degrade dietary proteins, resulting in small peptides. The peptides with high proline content, such as a gluten-derived peptide, are then cleaved by aminopeptidases including DPP IV [22]. DPP IV expression levels decreased in children with celiac disease, an immune-mediated enteropathy triggered by the ingestion of gluten in genetically predisposed individuals [12]. Additionally, recently, it has been proposed that the DPP IV-like activity of the intestinal microbiota contributes to protein digestion [22]. The retention of DPP IV in salivary EVs through the stomach until it reaches the intestine might aid in the digestion of dietary elements, together with intestinal DPP IV and the microbiota. Moreover, DPP IV has been thought to be involved in autoimmune diseases including inflammatory bowel disease, rheumatoid arthritis, and asthma [10,22]. DPP IV stimulates the proliferation of epithelial cells promotes the production of fibronectin [23]. It would be interesting to elucidate the relationship between the expression levels of DPP IV in salivary EVs and these diseases.

Inflammatory stimuli induce the generation and release of EVs bearing active proteins such as cytokines (i.e., IL-1, TNF-α, and IFN-β) and endoplasmic reticulum aminopeptidase 1 [5]. Since EVs/exosomes are now recognized as signal transduction complexes, salivary EVs might play a role in signal transduction by transferring active proteins when salivary glands are infected and/or become inflamed. The packaging of active components into salivary EVs and their continuous delivery throughout the gastrointestinal tract might facilitate their local actions in the tract. In this context, destabilized EVs might be recognized by the microfold (M) cells in the Peyer's patch to modulate mucosal immune system, when activated under infectious and/or inflammatory conditions. Further studies are required to elucidate the pathophysiological significance of the possible destabilization of salivary EVs under the simulated gastrointestinal conditions reported in this work.

5. Conclusion

Salivary EVs could pass through the stomach without undergoing significant damage, while they might be disrupted in the intestine to release their contents. However, some contents such as DPP IV may remain intact following digestion and solubilization in the gastrointestinal tract.

Declaration of competing interest

The authors declare that they have no known competing financial interests or personal relationships that could have appeared to influence the work reported in this paper.

The authors declare the following financial interests/personal relationships which may be considered as potential competing interests.

Acknowledgments

We are grateful to Sachie Matsubara and Junri Hayakawa (Laboratory for Electron Microscopy, Kyorin University School of Medicine) for their experimental assistance with electron microscopy. We would like to thank Dr. Nahoko Kumeda, Yuki Yamazaki, Nao Kobayashi, Kanako Takahashi, and Rina Miura (Faculty of Pharmaceutical Sciences, Teikyo Heisei University) for their experimental assistance. We would also like to thank Editage (www.editage.com) for English language editing.

Appendix A. Supplementary data

Supplementary data to this article can be found online at https://doi.org/10.1016/j.bbrep.2021.101034.

Funding

This work was supported in part by Grants-in-Aid from the Ministry of Education, Culuture, Sports, Science and Technology (Projects 16K08348 and 20K07162).

Role of the funding source

The funding source had no role in experimental design and execution, data analysis, and decision to submit results.

Authors' contributions

Yuko Ogawa: conceptualization; data curation; formal analysis, funding acquisition; methodology; validation; visualization; writing – review & editing. Yoshihiro Akimoto: investigation; resources. Mamoru Ikemoto: data curation; formal analysis. Yoshikuni Goto: data curation; formal analysis; resources. Anna Ishikawa: investigation. Sakura Ohta: investigation. Yumi Takase: investigation. Hayato Kawakami: resources. Masafumi Tsujimoto: conceptualization; writing – review & editing. Ryohei Yanoshita: conceptualization; project administration; supervision; validation; writing – review & editing.

Data availability statement

The authors confirm that the data supporting the findings of this study are available within the article and its supplementary materials.

References

[1] C. Thery, K.W. Witwer, E. Aikawa, C. Théry, K.W. Witwer, E. Aikawa, M.J. Alcaraz, J.D. Anderson, R. Andriantsitohaina, A. Antoniou, T. Arab, F. Archer, G.K. Atkin-Smith, D.C. Ayre, J.-M. Bach, D. Bachurski, L. Balaj, S. Baldacchino, N.N. Bauer, A. A. Baxter, M. Bebawy, C. Beckham, A.B. Zavec, A. Benmoussa, A.C. Berardi, P. Bergese, E. Bielska, C. Blenkiron, S. Bobis-Wozowicz, E. Boilard, W. Boireau, A. Bongiovanni, F.E. Borràs, S. Bosch, C.M. Boulanger, X. Breakefield, A.M. Breglio, M.Á. Brennan, D.R. Brigstock, A. Brisson, M.L.D. Broekman, J.F. Bromberg, P. Bryl-Górecka, S. Buch, A.H. Buck, D. Burger, S. Busatto, D. Buschmann, B. Bussolati, E. I. Buzás, J.B. Byrd, G. Camussi, D.R.F. Carter, S. Caruso, L.W. Chamley, Y.-T. Chang, C. Chen, S. Chen, L. Cheng, A.R. Chin, A. Clayton, S.P. Clerici, A. Cocks, E. Cocucci, R.J. Coffey, A. Cordeiro-da-Silva, Y. Couch, F.A.W. Coumans, B. Coyle, R. Crescitelli, M.F. Criado, C.D. 'Souza-Schorey, S. Das, A.D. Chaudhuri, P. de Candia, E.F. De Santana Jr., O. De Wever, H.A. del Portillo, T. Demaret, S. Deville, A. Devitt, B. Dhondt, D. Di Vizio, L.C. Dieterich, V. Dolo, A.P.D. Rubio, M. Dominici, M.R. Dourado, T.A.P. Driedonks, F.V. Duarte, H.M. Duncan, R. M. Eichenberger, K. Ekström, S.E.L. Andaloussi, C. Elie-Caille, U. Erdbrügger, J. M. Falcón-Pérez, F. Fatima, J.E. Fish, M. Flores-Bellver, A. Försönits, A. Frelet-Barrand, F. Fricke, G. Fuhrmann, S. Gabrielsson, A. Gámez-Valero, C. Gardiner, K. Gärtner, R. Gaudin, Y.S. Gho, B. Giebel, C. Gilbert, M. Gimona, I. Giusti, D.C. I. Goberdhan, A. Görgens, S.M. Gorski, D.W. Greening, J.C. Gross, A. Gualerzi, G. N. Gupta, D. Gustafson, A. Handberg, R.A. Haraszti, P. Harrison, H. Hegyesi, A. Hendrix, A.F. Hill, F.H. Hochberg, K.F. Hoffmann, B. Holder, H. Holthofer, B. Hosseinkhani, G. Hu, Y. Huang, V. Huber, S. Hunt, A.G.-E. Ibrahim, T. Ikezu, J. M. Inal, M. Isin, A. Ivanova, H.K. Jackson, S. Jacobsen, S.M. Jay, M. Jayachandran, G. Jenster, L. Jiang, S.M. Johnson, J.C. Jones, A. Jong, T. Jovanovic-Talisman, S. Jung, R. Kalluri, S.-I. Kano, S. Kaur, Y. Kawamura, E.T. Keller, D. Khamari, E. Khomyakova, A. Khvorova, P. Kierulf, K.P. Kim, T. Kislinger, M. Klingeborn, D. J. Klinke II, M. Kornek, M.M. Kosanović, Á.F. Kovács, E.-M. Krämer-Albers, S. Krasemann, M. Krause, I.V. Kurochkin, G.D. Kusuma, S. Kuypers, S. Laitinen, S. M. Langevin, L.R. Languino, J. Lannigan, C. Lässer, L.C. Laurent, G. Lavieu, E. Lázaro-Ibáñez, S.L. Lay, M.-S. Lee, Y.X.F. Lee, D.S. Lemos, M. Lenassi, A. Leszczynska, I.T.S. Li, K. Liao, S.F. Libregts, E. Ligeti, R. Lim, S.K. Lim, A. Linē, K. Linnemannstöns, A. Llorente, C.A. Lombard, M.J. Lorenowicz, Á.M. Lörincz, J. Lötvall, J. Lovett, M.C. Lowry, X. Loyer, Q. Lu, B. Lukomska, T.R. Lunavat, S.L. N. Maas, H. Malhi, A. Marcilla, J. Mariani, J. Mariscal, E.S. Martens-Uzunova, L. Martin-Jaular, M.C. Martinez, V.R. Martins, M. Mathieu, S. Mathivanan, M. Maugeri, L.K. McGinnis, M.J. McVey, D.G. Meckes Jr., K.L. Meehan, I. Mertens, V.R. Minciacchi, A. Möller, M.M. Jørgensen, A. Morales-Kastresana, J. Morhayim, F. Mullier, M. Muraca, L. Musante, V. Mussack, D.C. Muth, K.H. Myburgh, T. Najrana, M. Nawaz, I. Nazarenko, P. Nejsum, C. Neri, T. Neri, R. Nieuwland, L. Nimrichter, J.P. Nolan, E.N.M.N. Hoen, N.N. Hooten, L. O'Driscoll, T. O'Grady, A. O'Loghlen, T. Ochiya, M. Olivier, A. Ortiz, L.A. Ortiz, X. Osteikoetxea, O. Østergaard, M. Ostrowski, J. Park, D.M. Pegtel, H. Peinado, F. Perut, M. W. Pfaffl, D.G. Phinney, B.C.H. Pieters, R.C. Pink, D.S. Pisetsky, E.P. von Strandmann, I. Polakovicova, I.K.H. Poon, B.H. Powell, I. Prada, L. Pulliam, P. Quesenberry, A. Radeghieri, R.L. Raffai, S. Raimondo, J. Rak, M.I. Ramirez, G. Raposo, M.S. Rayyan, N. Regev-Rudzki, F.L. Ricklefs, P.D. Robbins, D. D. Roberts, S.C. Rodrigues, E. Rohde, S. Rome, K.M.A. Rouschop, A. Rughetti, A. E. Russell, P. Saá, S. Sahoo, E. Salas-Huenuleo, C. Sánchez, J.A. Saugstad, M.J. Saul, R.M. Schiffelers, R. Schneider, T.H. Schøyen, A. Scott, E. Shahaj, S. Sharma, O. Shatnyeva, F. Shekari, G.V. Shelke, A.K. Shetty, K. Shiba, P.R.-M. Siljander, A. M. Silva, A. Skowronek, O.L. Snyder II, R.P. Soares, B.W. Sódar, C. Soekmadji, J. Sotillo, P.D. Stahl, W. Stoorvogel, S.L. Stott, E.F. Strasser, S. Swift, H. Tahara, M. Tewari, K. Timms, S. Tiwari, R. Tixeira, M. Tkach, W.S. Toh, R. Tomasini, A. C. Torrecilhas, J.P. Tosar, V. Toxavidis, L. Urbanelli, P. Vader, B.W.M. van Balkom, S.G. van der Grein, J.V. Deun, M.J.C. van Herwijnen, K.V. Keuren-Jensen, G. van Niel, M.E. van Royen, A.J. van Wijnen, M.H. Vasconcelos, I.J. Vechetti Jr., T. D. Veit, L.J. Vella, É. Velot, F.J. Verweij, B. Vestad, J.L. Viñas, T. Visnovitz, K. V. Vukman, J. Wahlgren, D.C. Watson, M.H.M. Wauben, A. Weaver, J.P. Webber, V. Weber, A.M. Wehman, D.J. Weiss, J.A. Welsh, S. Wendt, A.M. Wheelock, Z. Wiener, L. Witte, J. Wolfram, A. Xagorari, P. Xander, J. Xu, X. Yan, M. Yáñez-Mó, H. Yin, Y. Yuana, V. Zappulli, J. Zarubova, V. Žėkas, J.-Y. Zhang, Z. Zhao, L. Zheng, A.R. Zheutlin, Minimal information for studies of extracellular vesicles 2018 (MISEV2018): a position statement of the International Society for Extracellular Vesicles and update of the MISEV2014 guidelines, J. Extracell. Vesicles 7 (2018), 1535750, https://doi.org/10.1080/20013078.2018.1535750.

[2] G. Raposo, W. Stoorvogel, Extracellular vesicles: exosomes, microvesicles, and friends, J. Cell Biol. 200 (2013) 373–383, https://doi.org/10.1083/jcb.201211138.

[3] C.S. Lau, D.T. Wong, Breast cancer exosome-like microvesicles and salivary gland cells interplay alters salivary gland cell-derived exosome-like microvesicles in vitro, PloS One 7 (2012), e33037, https://doi.org/10.1371/journal.pone.0033037.

[4] J.S. Byun, S.H. Hong, J.K. Choi, J.-K. Jung, H.-J. Lee, Diagnostic profiling of salivary exosomal microRNAs in oral lichen planus patients, Oral Dis. 21 (2015) 987–993, https://doi.org/10.1111/odi.12374.

[5] Y. Goto, Y. Ogawa, H. Tsumoto, Y.Y. Miura, T.J. Nakamura, K. Ogawa, Y. Akimoto, H. Kawakami, T. Endo, R. Yanoshita, M. Tsujimoto, Contribution of the exosome-associated form of secreted endoplasmic reticulum aminopeptidase 1 to exosome-mediated macrophage activation, Biochim. Biophys. Acta Mol. Cell Res. 1865 (2018) 874–888, https://doi.org/10.1016/j.bbamcr.2018.03.009.

[6] Y. Ogawa, Y. Miura, A. Harazono, M. Kanai-Azuma, Y. Akimoto, H. Kawakami, T. Yamaguchi, T. Toda, T. Endo, M. Tsubuki, R. Yanoshita, Proteomic analysis of two types of exosomes in human whole saliva, Biol. Pharm. Bull. 34 (2011) 13–23, https://doi.org/10.1248/bpb.34.13.

[7] Y. Ogawa, M. Kanai-Azuma, Y. Akimoto, H. Kawakami, R. Yanoshita, Exosome-like vesicles in Gloydius blomhoffii venom, Toxicon 51 (2008) 984–993, https://doi.org/10.1016/j.toxicon.2008.02.003.

[8] Y. Ogawa, M. Kanai-Azuma, Y. Akimoto, H. Kawakami, R. Yanoshita, Exosome-like vesicles with dipeptidyl peptidase IV in human saliva, Biol. Pharm. Bull. 31 (2008) 1059–1062, https://doi.org/10.1248/bpb.31.1059.

[9] N. Kumeda, Y. Ogawa, Y. Akimoto, H. Kawakami, M. Tsujimoto, R. Yanoshita, Characterization of membrane integrity and morphological stability of human salivary exosomes, Biol. Pharm. Bull. 40 (2017) 1183–1191, https://doi.org/10.1248/bpb.b16-00891.

[10] A.M. Lambeir, C. Durinx, S. Scharpe, I. De Meester, Dipeptidyl-peptidase IV from bench to bedside: an update on structural properties, functions, and clinical aspects of the enzyme DPP IV, Crit. Rev. Clin. Lab Sci. 40 (2003) 209–294, https://doi.org/10.1080/713609354.

[11] N. Kandzija, W. Zhang, C. Motta-Mejia, V. Mhlomi, J. McGowan-Downey, T. James, A.S. Cerdeira, D. Tannetta, I. Sargent, C.W. Redman, C.C. Bastie, M. Vatish, Placental extracellular vesicles express active dipeptidyl peptidase IV; levels are increased in gestational diabetes mellitus, J. Extracell. Vesicles 8 (2019) 1617000, https://doi.org/10.1080/20013078.2019.1617000.

[12] D. Detel, M. Persic, J. Varljen, Serum and intestinal dipeptidyl peptidase IV (DPP IV/CD26) activity in children with celiac disease, J. Pediatr. Gastroenterol. Nutr. 45 (2007) 65–70, https://doi.org/10.1097/MPG.0b013e318054b085.

[13] G. Janssen, C. Christis, Y. Kooy-Winkelaar, L. Edens, D. Smith, P. van Veelen, F. Koning, Ineffective degradation of immunogenic gluten epitopes by currently available digestive enzyme supplements, PloS One 10 (2015), e0128065, https://doi.org/10.1371/journal.pone.0128065.

[14] S. Boukouris, S. Mathivanan, Exosomes in bodily fluids are a highly stable resource of disease biomarkers, Proteonomics Clin. Appl. 9 (2015) 358–367, https://doi.org/10.1002/prca.201400114.

[15] Y. Liao, X. Du, J. Li, B. Lonnerdal, Human milk exosomes and their microRNAs survive digestion in vitro and are taken up by human intestinal cells, Mol. Nutr. Food Res. 61 (2017), 1700082, https://doi.org/10.1002/mnfr.201700082.

[16] J. Van Deun, P. Mestdagh, P. Agostinis, Ö. Akay, S. Anand, J. Anckaert, Z. A. Martinez, T. Baetens, E. Beghein, L. Bertier, G. Berx, J. Boere, S. Boukouris, M. Bremer, D. Buschmann, J.B. Byrd, C. Casert, L. Cheng, A. Cmoch, Delphine Daveloose, Eva De Smedt, Seyma Demirsoy, Victoria Depoorter, Bert Dhondt, T.A.P. Driedonks, A. Dudek, A. Elsharawy, I. Floris, A.D. Foers, K. Gärtner, A.D. Garg, E. Geeurickx, J. Gettemans, F. Ghazavi, B. Giebel, T. G. Kormelink, G. Hancock, H. Helsmoortel, A.F. Hill, V. Hyenne, H. Kalra, D. Kim, J. Kowal, S. Kraemer, P. Leidinger, C. Leonelli, Y. Liang, L. Lippens, S. Liu, A. Lo Cicero, S. Martin, S. Mathivanan, P. Mathiyalagan, T. Matusek, G. Milani, M. Monguió-Tortajada, L.M. Mus, D.C. Muth, A. Németh, E.N.M. Nolte-'t Hoen, L. O'Driscoll, R. Palmulli, M.W. Pfaffl, B. Primdal-Bengtson, E. Romano, Q. Rousseau, S. Sahoo, N. Sampaio, M. Samuel, B. Scicluna, B. Soen, A. Steels, J. V. Swinnen, M. Takatalo, S. Thaminy, C. Théry, J. Tulkens, I. Van Audenhove, S. van der Grein, A. Van Goethem, M.J. van Herwijnen, G. Van Niel, N. Van Roy, A. R. Van Vliet, N. Vandamme, S. Vanhauwaert, G. Vergauwen, F. Verweij, A. Wallaert, M. Wauben, K.W. Witwer, M.I. Zonneveld, O. De Wever, J. Vandesompele, A. Hendrix, Ev-track: transparent reporting and centralizing knowledge in extracellular vesicle research, Nat. Methods 14 (2017) 228–232, https://doi.org/10.1038/nmeth.4185.

[17] J.P. Hamilton, G. Xie, J.P. Raufman, S. Hogan, T.L. Griffin, C.A. Packard, D. A. Chatfield, L.R. Hagey, J.H. Steinbach, A.F. Hofmann, Human cecal bile acids: concentration and spectrum, Am. J. Physiol. Gastrointest. Liver Physiol. 293 (2007) G256–G263, https://doi.org/10.1152/ajpgi.00027.2007.

[18] T.C. Northfield, I. McColl, Postprandial concentrations of free and conjugated bile acids down the length of the normal human small intestine, Gut 14 (1973), https://doi.org/10.1136/gut.14.7.513, 513-158.

[19] E. London, D.A. Brown, Insolubility of lipids in triton X-100: physical origin and relationship to sphingolipid/cholesterol membrane domains (rafts), Biochim. Biophys. Acta 1508 (2000) 182–195, https://doi.org/10.1016/s0304-4157(00)00007-1.

[20] B.J. Underdown, K.J. Dorrington, Studies on the structural and conformational basis for the relative resistance of serum and secretory Immunoglobulin A to proteolysis, J. Immunol. 112 (1974) 949–959.

[21] G. van Niel, G. Raposo, C. Candalh, M. Boussac, R. Hershberg, N. Cerf-Bensussan, M. Heyman, Intestinal epithelial cells secrete exosome-like vesicles, Gastroenterology 121 (2001) 337–349, https://doi.org/10.1053/gast.2001.26263.

[22] M. Olivares, V. Schüppel, A. Hassan M., M. Beaumont, A. Neyrinck M., L. Bindels B., A. Benítez-Páez, Y. Sanz, D. Haller, P. Holzer, N. Delzenne M., The Potential Role of the Dipeptidyl Peptidase-4-Like Activity From the Gut Microbiota on the Host Health, Front Microbiol. 9 (2018) 1900, https://doi.org/10.3389/fmicb.2018.01900.

[23] T. Shiobara, K. Chibana, T. Watanabe, R. Arai, Y. Horigane, Y. Nakamura, Y. Hayashi, Y. Shimizu, A. Takemasa, Y. Ishii, Dipeptidyl peptidase-4 is highly expressed in bronchial epithelial cells of untreated asthma and it increases cell proliferation along with fibronectin production in airway constitutive cells, Respir. Res. 17 (2016) 28, https://doi.org/10.1186/s12931-016-0342-7.